THE JOURNAL OF BIOLOGICAL CHEMISTRY VOL. 291, NO. 20, pp. 10551–10561, May 13, 2016

Human and Murine Interleukin 23 Receptors Are Novel Substrates for A Disintegrin and Metalloproteases ADAM10 and ADAM17*

Received for publication, December 14, 2015, and in revised form, February 29, 2016 Published, JBC Papers in Press, March 9, 2016, DOI 10.1074/jbc.M115.710541

Manuel Franke[‡], Jutta Schröder[‡], Niloufar Monhasery[‡], Theresa Ackfeld[‡], Thorben M. Hummel[‡], Björn Rabe[§], Christoph Garbers[§], Christoph Becker-Pauly[§], Doreen M. Floss[‡], and Jürgen Scheller[‡1]

From the [‡]Institute of Biochemistry and Molecular Biology II, Medical Faculty, Heinrich-Heine-University, 40225 Düsseldorf, Germany and the [§]Institute of Biochemistry, Kiel University, 24098 Kiel, Germany

IL-23 (interleukin 23) regulates immune responses against pathogens and plays a major role in the differentiation and maintenance of T_H17 cells and the development of autoimmune diseases and cancer. The IL-23 receptor (IL-23R) complex consists of the unique IL-23R and the common IL-12 receptor $\beta1$ (IL-12R$\beta1$). Differential splicing generates antagonistic soluble IL-23R (sIL-23R) variants, which might limit IL-23-mediated immune responses. Here, ectodomain shedding of human and murine IL-23R was identified as an alternative pathway for the generation of sIL-23R. Importantly, proteolytically released sIL-23R has IL-23 binding activity. Shedding of IL-23R was induced by stimulation with the phorbol ester phorbol 12-myristate 13-acetate (PMA), but not by ionomycin. PMA-induced shedding was abrogated by an ADAM (A disintegrin and metalloprotease) 10 and 17 selective inhibitor, but not by an ADAM10 selective inhibitor. ADAM17-deficient but not ADAM10-deficient HEK293 cells failed to shed IL-23R after PMA stimulation, demonstrating that ADAM17 but not ADAM10 cleaves the IL-23R. Constitutive shedding was, however, inhibited by an ADAM10 selective inhibitor. Using deletions and specific amino acid residue exchanges, we identified critical determinants of ectodomain shedding within the stalk region of the IL-23R. Finally, interaction studies identified domains 1 and 3 of the IL-23R as the main ADAM17 binding sites. In summary, we describe human and murine IL-23R as novel targets for protein ectodomain shedding by ADAM10 and ADAM17.

The pro-inflammatory cytokine IL-23 is composed of the IL-12p40 subunit and p19 (1). IL-23 is a key factor for the development of T_H17 cells (2), which control antimicrobial and antifungal responses, but is also critically involved in the pathogenesis of chronic inflammatory disorders (3). The receptor complex is composed of the common IL-12 receptor $\beta1$ (IL-12 $\beta1$),[2] shared with IL-12, and the unique IL-23 receptor (4, 5). Single nucleotide polymorphisms within the *IL23R* gene were associated with various autoimmune diseases and the risk to develop cancer (1). Upon recruitment of the receptors by IL-23, which results in a noncanonical receptor complex formation (6), signaling is initiated by activation of associated Tyk2 (tyrosine kinase 2) and Jak2 (Janus kinase 2), which phosphorylate predominantly STAT3, and to a lesser extent STAT1, STAT4, and STAT5 (5). Recently, a noncanonical tyrosine-independent STAT3 activation site within the IL-23R was identified (7). In addition to STAT proteins PI3K, MAPK and NF-κB signaling pathways were activated (7, 28).

Ectodomain shedding of membrane-bound proteins leads to receptor protein down-regulation on the cell surface and the generation of soluble protein ectodomains with agonistic or antagonistic properties. Members of the ADAM (A disintegrin and metalloprotease) gene family are major ectodomain shedding proteinases. ADAM17 and its close relative ADAM10 are the major sheddases of this family, (8), with extensive overlap and compensation for several substrates, including EGF receptor ligands, TNF, TNF receptor, and IL-6R (9, 10). Activation of ADAM proteases is achieved by different stimuli including phorbol ester (phorbol-12-myristate-13-acetate (PMA)), ionomycin, ligands of G-protein-coupled receptors, ATP, bacterial toxins, bacterial metalloproteinases, and apoptosis (8). For some ADAM target proteins such as Notch, induction of intracellular signaling by the remaining intracellular domain cleavage product has been described (11). Previously, it was shown that alternative splicing of IL-23R result in a series of truncated soluble IL-23R proteins (12–14).

Here, we discovered murine and human IL-23R as novel substrates of ADAM10 and ADAM17, resulting in the release of soluble IL-23R proteins, which retained their ability to bind to IL-23. Distinct areas within the murine and human IL-23R, which are important for ectodomain shedding, were identified in murine and human IL-23R. Immunoprecipitation analysis revealed domains 1 and 3 of IL-23R as critical ADAM17 interaction sites. Thus, we propose that ectodomain shedding is a second mechanism that contributes to the generation of soluble IL-23R variants.

* This work was funded by grants from the Deutsche Forschungsgemeinschaft, Bonn, Germany (DFG SCHE907/3–1 to J. S., SFB877 project A9 to C. B.-P. and A10 to C. G.). The authors declare that they have no conflicts of interest with the contents of this article.

[1] To whom correspondence should be addressed: Inst. of Biochemistry and Molecular Biology II, Medical Faculty, Heinrich-Heine-University, Universitätsstr. 1, 40225 Düsseldorf, Germany. Fax: 49-2118112726; E-Mail: jscheller@uni-duesseldorf.de.

[2] The abbreviations used are: IL-23R, IL-23 receptor; ADAM, A disintegrin and metalloprotease; sIL-23R, soluble IL-23R; PMA, phorbol 12-myristate 13-acetate; IL-6R, IL-6 receptor; aa, amino acid(s); GI, GI254023X; GW, GW280264X.

Experimental Procedures

Cells and Reagents—Ba/F3-gp130-mIL-12Rβ1 and Ba/F3-gp130-mIL-12Rβ1-mIL-23R cells and the packaging cell line Phoenix-Eco were described previously (7). HEK293 (ACC 305), HEK293T (ATCC CRL-3216), and COS-7 (ACC-60) cells were from DSMZ (Deutsche Sammlung von Mikrorganismen und Zellkulturen GmbH) (Braunschweig, Germany). To generate ADAM10- and ADAM17-deficient HEK293T cells, CRISPR/Cas9 plasmids (based on LeGO-Cas9, a kind gift of Boris Fehse, UKE Hamburg, Germany) were transfected into HEK293T cells using TurboFect transfection reagent (Life Technologies). Successfully transfected cells were enriched by a 48-h selection with 1 μg/ml puromycin. To obtain ADAM10/ADAM17 double knock-out cells LeGO-Cas9-ADAM10-transfected cells were transfected with LeGO-Cas9-ADAM17 2 weeks after the first transfection. For the isolation of single genome-edited cells, cell populations were subjected to flow cytometry after immunostaining with PE anti-human CD156c antibody (BioLegend, San Diego, CA) and A300E antibody (Institute of Biochemistry, Kiel, Germany), and single protease-deficient cells were sorted into 96-well plates. HEK293T cell lines with CRISPR/Cas9-mediated knock-out of ADAM10, ADAM17, or both are described in detail by Riethmueller *et al.*[3] All cell lines were grown in DMEM high glucose culture medium (Gibco®, Life Technologies) supplemented with 10% fetal calf serum, penicillin (60 mg/liter), and streptomycin (100 mg/liter) (Genaxxon Bioscience, Ulm, Germany) at 37 °C with 5% CO_2 in a water-saturated atmosphere. The medium for Ba/F3 cell lines was supplemented with 10 ng/ml Hyper-IL-6, a fusion protein of IL-6 and the soluble IL-6R, which is a mimic of IL-6 trans-signaling (15). Biotinylated mouse IL-23R antibody (BAF1686), streptavidin-HRP, monoclonal mouse IL-23R antibody (MAB1686), and biotinylated human IL-23R antibody (BAF1400) were from R&D Systems (Minneapolis, MN). The monoclonal GFP antibody was purchased by Roche. Anti-mouse IgG-POD was from Thermo Fisher Scientific. The Alexa Fluor 647-conjugated goat anti-rat IgG was from Jackson ImmunoResearch Laboratories (Dianova, Hamburg, Germany). APC-streptavidin was from BD Biosciences. PMA and ionomycin were purchased from Sigma-Aldrich. Marimastat was from Sigma-Aldrich. The two metalloprotease inhibitors GI254023X (GI, selective for ADAM10) and GW280264X (GW, selective for both ADAM10 and ADAM17) were from Iris Biotech (Marktredwitz, Germany) (16).

Construction of Expression Plasmids—Plasmids containing the coding sequences for hIL-23R and hIL-12Rβ1 were obtained from Esther van de Vosse (Leiden University Medical Center, Leiden, The Netherlands) (17, 18) and cloned into p409 (19) for transient transfection of HEK293 cells and into the retroviral plasmids pMOWS-puro or pMOWS-hygro (20) for generation of stable Ba/F3-gp130 cell lines. The eukaryotic expression plasmid for mIL-23R was described (7) and used as template for cloning of stalk deletion variants. Human and murin IL-23R deletion cDNA variants and the IL-23R-(stalk hIL-6R)-chimeric cDNA were constructed using standard cloning procedures via splicing by overlapping extension PCRs and subcloned into p409. As mentioned above, cDNAs for hIL-23R variants were additionally subcloned into the pMOWS-puro plasmid and hIL-12Rβ1 into the pMOWS-hygro plasmid for retroviral transduction of Ba/F3-gp130 cells (7). The resulting cDNAs for mIL-23R variants were inserted into the pMOWS-puro vector and used for the retroviral transduction of Ba/F3-gp130-mIL-12Rβ1 cells. Mutations of valine within the putative murine ADAM17 cutting region of mIL-23R (V342D, V339D, and V339D/V342D) were introduced by PCR using Phusion® high fidelity DNA polymerase (FINNZYMES, Thermo Fisher Scientific) followed by DpnI digestion of methylated template DNA. The coding sequence of Hyper-IL-23, a fusion protein of murine p40 followed by a synthetic linker (RGGGGSGGGGSVE) and murine p19 (21) was C-terminally fused with human Fc tag to generate Hyper-IL-23Fc (HIL-23Fc). Furthermore, human Fc was fused to the C terminus of murine IL-23R containing amino acids 24–315 using standard cloning procedures to obtain the mIL23R D1D2D3-Fc fusion protein (6). Accordingly, mIL-23R D1D2-Fc (aa 24–217) and IL-23R D1-Fc (aa 24–123) have been generated. Splicing by overlapping extension PCRs was used to generate expression plasmids for mIL-23R D2D3-Fc (aa 122–315), mIL-23R D2-Fc (aa 122–217), and mIL-23R D3-Fc (aa 218–315), respectively. ADAM17-GFP was cloned in our group by PCR amplification of murine ADAM17 and C-terminally fusing the PCR product in the open reading frame of GFP.

Transfection, Transduction, and Selection of Cells—Transient transfection of HEK293 and COS-7 cells was performed using TurboFect (Fermentas, Thermo Fisher Scientific) according to the manufacturer's instructions. Retroviral transduction of Ba/F3-gp130 cells was performed as described previously (7). Ba/F3-gp130 cells were retrovirally transduced to obtain Ba/F3-gp130 cell lines expressing hIL-12Rβ1 and wild-type murine or human hIL-23R or variants thereof.

Shedding Assays—To analyze IL-23R ectodomain shedding in stably transduced Ba/F3-gp130-IL-12Rβ1-IL-23R cells, the cells were washed once with PBS and diluted to a concentration of 1.2×10^6/ml. The cells were incubated with the inhibitors GI254023X (GI) or GW280264X (GW) for 30 min and afterward for 2 h with PMA (100 nM) or 1 h with ionomycin (1 μM). For constitutive shedding, the cells were incubated for 24 h with GI (3 μM), GW (3 μM), Marimastat (10 μM), or DMSO, which was added after 3 and 6 h. Cell supernatants were centrifuged to remove cellular debris. A volume of 1 ml of each supernatant was then incubated overnight at 4 °C under constant agitation with 1 ml of supernatant of COS-7 cells and transiently transfected with the cDNA coding for HIL-23Fc to bind soluble IL-23R (sIL-23R). Afterward the complex was incubated with protein A-agarose for 4 h at 4 °C under constant agitation. The agarose beads were then collected by centrifugation, and the supernatant was removed. The beads were washed two times with ice-cold IP buffer (20 mM Tris-HCl, pH 7.5, 150 mM NaCl, 1 mM EDTA, 1 mM EGTA, 2.5 mM sodium pyrophosphate, 1 mM β-glycerophosphate, 1 mM Na_3VO_4, and a complete protease inhibitor mixture tablet/50 ml buffer (Roche Diagnostics)) and directly boiled in Laemmli buffer, which was subsequently

[3] S. Riethmueller, J. C. Ehlers, J. Lokau, S. Düsterhöft, K. Knittler, G. Dombrowsky, J. Grötzinger, B. Rabe, S. Rose-John, and C. Garbers, submitted for publication.

analyzed by Western blot. To investigate ectodomain shedding of IL-23R in transiently transfected HEK293 cells, the cells were seeded out at 1×10^6/ml 24 h after transfection. Shedding assays were performed as described for Ba/F3 cells.

Flow Cytometry—For detection of cell surface expression of the different murine IL-23R variants, 1×10^6 Ba/F3-gp130-IL-12Rβ1-IL-23R cell lines were washed once with FACS buffer (PBS, 0.5% BSA) and incubated with 2.5 μg of monoclonal mouse IL-23R antibody for 1 h on ice. After three subsequent washing steps with FACS buffer, the cells were incubated in 100 μl of FACS buffer containing a 1:100 dilution of Alexa Fluor 647-conjugated Fab goat anti-rat IgG for 1 h at 4 °C. The cells were washed with FACS buffer, resuspended in 500 μl of FACS buffer, and analyzed by flow cytometry on a BD Bioscience FACS Canto II. The resulting data were evaluated using the FCS Express software (De Novo Software, Los Angeles, CA). Human IL-23R surface expression was detected with 0.5 μg of human IL-23R-biotinylated monoclonal antibody/100 μl of FACS buffer followed by incubation with 0.2 μg of APC-streptavidin/100 μl of FACS buffer.

Expression and Purification of GFP Nanobodies—The GFP nanobody (V_HH) used for co-immunoprecipitation was designed according to (22). A C-terminal myc and His_6 tag was fused to the GFP-binding V_HH domain, cloned into pET23a-PelB vector, and transformed in component *Escherichia coli* BL21 cells. 2 liters of culture medium was inoculated with 50 ml of *E. coli* preculture and incubated at 37 °C and 140 rpm to an A_{600} of 0.8. Bacterial expression was induced with 1 mM isopropyl β-D-1-thiogalactopyranoside, and the cells were incubated overnight at 30 °C and 140 rpm. The cells were removed by centrifugation (1 h, 4 °C, 3000 $\times$ *g*), and supernatant was subjected to purification. Bacterial supernatant was filtered by a 0.45-μm SCFA NALGENE® Rapid-Flow™ bottle top filter (Thermo Fisher Scientific) to remove cell debris, mixed 1:1 with PP buffer (500 mM NaCl, 50 mM Na_2HPO_4/NaH_2PO_4, pH 7.4), and loaded on a pre-equilibrated nickel-nitrilotriacetic acid column (His-Trap FF; GE Healthcare). His-tagged GFP nanobodies were eluted by PP buffer containing 500 mM imidazole. After removal of imidazole the purified protein was concentrated using Amicon® Ultra-15 10K centrifugal filter devices (Merck Millipore).

Coupling of GFP Nanobody to Sepharose Beads—For coupling of the purified GFP nanobodies to Sepharose, 1 mg of purified GFP nanobodies were covalently linked to 2 ml of NHS-activated Sepharose 4 Fast Flow (Ge Healthcare), according to the manufacturer's instructions. Therefore, beads were washed three times with ice-cold 1 mM HCl (2 min, 3000 $\times$ *g*, 4 °C). Purified protein was added to the beads and incubated for 2 h at room temperature under constant agitation. By adding blocking buffer (0.5 ethanolamine, 0.5 NaCl, pH 8.3) for 2 h under constant agitation, remaining free binding sites were blocked. Finally, beads were washed twice with 0.1 M Tris-HCl, pH 8, and stored in 20% ethanol at 4 °C.

Co-immunoprecipitation of IL-23R and ADAM17—Interaction of ADAM17 and IL-23R was analyzed by co-immunoprecipitation. Therefore, HEK293 cells were co-transfected with murine ADAM17-GFP and the corresponding IL-23R variant. 48 h after transfection, the cells were lysed in lysis buffer (20 mM Tris-HCl, pH 7.5, 150 mM NaCl, 0.5 mM EDTA, 0.5% Nonidet P-40 (Tergitol-type Nonidet P-40) and a complete protease inhibitor mixture tablet/50 ml of buffer) for 1 h at 4 °C under constant agitation and centrifuged at 20000 $\times$ *g* for 20 min. The resulting cell lysate was mixed with 300 μl of dilution buffer (20 mM Tris-HCl, pH 7.5, 150 mM NaCl, 0.5 mM EDTA, and a complete protease inhibitor mixture tablet/50 ml of buffer). For input control (I), 50 μl of this solution was mixed with 50 μl of 5$\times$ Laemmli buffer and incubated for 10 min at 95 °C. Sepharose beads that were coupled with GFP nanobodies were washed twice with dilution buffer to remove the ethanol and subjected to the cell lysate mixture mentioned before. Beads and lysate were incubated at room temperature for 2 h under constant agitation to bind mADAM17-GFP to the GFP nanobody Sepharose beads. Afterward Sepharose beads were collected by centrifugation. 50 μl of resulting supernatant were mixed with Laemmli buffer and incubated for 10 min at 95 °C (referred to as nonbound). The beads were washed three times with ice-cold dilution buffer and finally directly boiled in Laemmli buffer. After centrifugation, the resulting supernatant was subsequently used for Western blotting referred to as bound fraction.

Western Blotting—25 μl of proteins from precipitated supernatant or cell lysate were separated by SDS-PAGE under reducing conditions and transferred to a PVDF membrane (GE Healthcare). The membranes were blocked with 5% skim milk powder in TBST-T (10 mM Tris-HCl, pH 7.6, 150 mM NaCl, and 0.05% Tween 20) and probed with the primary antibody in 5% skim milk powder in TBS-T (anti-human Fc, anti-GFP) or 5% BSA in TBS-T (hIL-23R biotinylated mAb, mIL-23R biotinylated mAb) at 4 °C overnight. After several washing steps, membranes were probed with the secondary peroxidase-conjugated antibody or streptavidin-HRP for 1 h at room temperature before applying the ECL Prime Western blotting detection reagent (GE Healthcare) according to the manufacturer´s instructions. To remove the antibodies, membranes were stripped in 62.5 mM Tris-HCl (pH 6.8), 2% SDS, and 0.1% β-mercaptoethanol for 20 min at 60 °C.

Internalization—2×10^6 Ba/F3-gp130-mIL-12Rβ1-mIL-23R cells were stimulated with Marimastat (10 μM), GI (3 μM), GW (3 μM), or DMSO for 30 min at 37 °C; washed with FACS buffer (0.5% BSA/PBS); and incubated with primary antibody (α-mIL-23R, α-hIL-23R) for 1 h on ice. Afterward the cells were resuspended in prewarmed medium supplemented with HIL-23 (0.2% of conditioned cell culture medium from a stable CHO-K1 cell line secreting HIL-23 (7)), Marimastat (10 μM), GI (3 μM), GW (3 μM), or DMSO and incubated for the indicated time points at 37 °C and 5% CO_2. Subsequently cells were washed and stored on ice. After the last time point, cells were incubated for 1 h on ice with secondary antibody (Alexa Fluor 647 conjugate). After removing the nonbound antibodies by washing, the cells were analyzed by flow cytometry on a BD Bioscience FACS Canto II, and the data were visualized using the FCS Express software.

Programs and Statistical Analysis—Western blots were analyzed by ImageJ. Statistical analysis was performed by using Student's *t* test. A *p* value of < 0.05 (*) was defined as statistically significant; $p < 0.01$ (**), $p < 0.001$ (***).

Results

Inhibition of Ectodomain Shedding Prolonged the Half-life of IL-23R on the Cell Surface—We analyzed the cell surface half-life of the murine IL-23R. Murine IL-23R cDNA was stably introduced into Ba/F3-gp130-mIL-12Rβ1 cells. Ba/F3 cells are ideal tools for determining the cell surface half-life of membrane proteins by flow cytometry (23). Cell surface expressed mIL-23R was labeled with IL-23R antibodies at 4 °C, and non-bound antibodies were washed away. Cells were shifted back to 37 °C for 0, 10, 20, 30, 60, and 90 min to allow IL-23R internalization and ectodomain shedding in the presence and absence of HIL-23. After the indicated time points, the cells were stained with secondary Alexa Fluor 647-conjugated Fab goat anti-rat IgG at 4 °C to quantify the remaining cell surface expression of IL-23R by flow cytometry. The time point T0 is the same in all experiments shown in Fig. 1*A* because the experiment for all conditions were done in parallel. During the flow cytometry pulse-chase experiment, the time-dependent reduction of cell surface IL-23R expression was analyzed. Cell surface half-life of mIL-23R in the presence and absence of HIL-23 was comparable with ~14 min without and ~18 min with cytokine stimulation (Fig. 1, *A* and *B*). Interestingly, inhibition of ectodomain shedding by GI, GW, or Marimastat resulted in prolonged cell surface exposition of IL-23R of ~28, 35, and 37 min, suggesting that disappearance of membrane-bound IL-23R was conducted by a combination of internalization and ectodomain shedding.

Induced Ectodomain Shedding of the IL-23R Is Mediated by ADAM17—Human and murine IL-23R cDNAs were stably introduced into Ba/F3-gp130-IL-12Rβ1 cells. Cell surface expression of human IL-23R (hIL-23R) was verified by flow cytometry (Fig. 2*A*). Proliferation of Ba/F3-gp130-IL-12Rβ1-IL-23R cells was dependent on IL-23, confirming biological activity of both IL-23 receptors (data not shown). Ba/F3-gp130-IL-12Rβ1-IL-23R cells were treated with PMA and ionomycin. Soluble IL-23R (sIL-23R) within the cellular supernatant was co-precipitated with HIL-23Fc fusion protein and protein A-agarose. Co-precipitated sIL-23R was detected by Western blotting. As depicted in Fig. 2*B*, human and murine sIL-23Rs were detected in the cell culture supernatant after PMA but almost not after ionomycin treatment. As control for the co-precipitation, HIL-23Fc was detected by Western blotting using an Fc-specific antibody. Typically PMA induces ADAM17, whereas ADAM10 is stimulated by ionomycin (9). Our results clearly demonstrate that sIL-23R was generated after PMA treatment, suggesting ectodomain shedding of the receptor. Next, Ba/F3-gp130-IL-12Rβ1 cells expressing human or murine IL-23R were treated with PMA in the presence of the ADAM10-selective inhibitor GI or the ADAM10/ADAM17-selective inhibitor GW (9). Again, PMA treatment resulted in release of sIL-23R, which was inhibited by GW but not by GI (Fig. 2*C*). These results suggest that ADAM17 is activated after PMA treatment and releases IL-23R by ectodomain shedding.

We have shown previously that the IL-6R stalk region is cleaved by ADAM17 after PMA stimulation and by ADAM10 after ionomycin stimulation (9). Because we did not observe ionomycin-induced shedding of the IL-23R, we asked whether transfer of the IL-6R stalk region results in ionomycin-induced shedding. We generated the synthetic hybrid receptor, consisting of human IL-23R extracellular domains (D1–D3), transmembrane domain, and the intracellular domain, with an interspersed exchange of the IL-23R stalk region by the IL-6R stalk domain. In transiently transfected HEK293 cells, the IL-23R-(stalk-IL-6R) chimeric receptor was cleaved after PMA stimulation with ADAM17, because GW completely suppressed the generation of sIL-23R, and interestingly, restored ionomycin-induced IL-23R shedding mediated by ADAM10 was completely suppressed by GI (Fig. 2, *D* and *E*), suggesting that the composition of the stalk region was sufficient to enable induction of ADAM10-induced shedding.

Even though we did not detect ionomycin-induced IL-23R shedding, we analyzed whether IL-23R is a substrate of constitutive shedding commonly mediated by ADAM10 (11). Equal numbers of Ba/F3-gp130-IL-12Rβ1 cells expressing human or murine IL-23R were incubated for 24 h without further stimulation, and sIL-23R was detected by HIL-23Fc co-precipitation and Western blotting. After 24 h, human and murine sIL-23R were detected in the supernatants of the cells (Fig. 2*F*). Interestingly, the broad spectrum inhibitor Marimastat, the ADAM10-selective inhibitor GI, and the ADAM10/ADAM17-selective inhibitor GW completely suppressed the generation of sIL-23R (Fig. 2*F*), suggesting that ADAM10 is the constitutive sheddase of IL-23R.

We also made use of HEK293T cells, transiently transfected with murine or human IL-23R cDNA, in which ADAM10, ADAM17, or both proteases were genetically inactivated by CRISPR/Cas9 targeting. Stimulation of PMA resulted in the formation of murine and human sIL-23R, which was completely absent in ADAM17- and ADAM10/ADAM17-deficient HEK293T cells but not in ADAM10 deficient cells. As a control, sIL-23R was detected in ADAM17-deficient HEK293T cells, which were reconstituted by transient transfection with a cDNA coding for murine ADAM17 (mADAM17-GFP fusion protein) (Fig. 2, *G* and *H*). Our results demonstrate that murine and human IL-23R were novel substrates of ADAM10 and ADAM17 and that the soluble receptors retained binding capacity toward IL-23 as approved by HIL-23Fc co-precipitation.

Generation of Noncleavable IL-23R Variants by Deletions or Amino Acids Exchanges within the Stalk Region of IL-23R—The IL-23R consists of three extracellular domains for cytokine binding (6): the relatively long most probably unstructured stalk region, the transmembrane domain, and the intracellular domain, responsible for execution of signal transduction (7). Substrate cleavage by ADAM proteases often occurs in close proximity to the cellular membrane (11). By stepwise deletion of amino acid residues within the IL-23R stalk region, we aimed to narrow down the ADAM17 cleavage side within the IL-23R. Four stalk deletion variants of murine IL-23R were generated (mIL-23RΔ363–372, mIL-23RΔ353–372, mIL-23RΔ343–372, and mIL-23RΔ333–372) (Fig. 3*A*) and stably transduced in Ba/F3-gp130-mIL-12Rβ1 cells. Cell surface expression of mIL-23RΔ363–372, mIL-23RΔ353–372, mIL-23RΔ343–372, and mIL-23RΔ333–372 was verified by flow cytometry (Fig. 3*B*). Shedding of mIL-23RΔ363–372, mIL-23RΔ353–372, and mIL-23RΔ343–372 after PMA stimulation was comparable with the

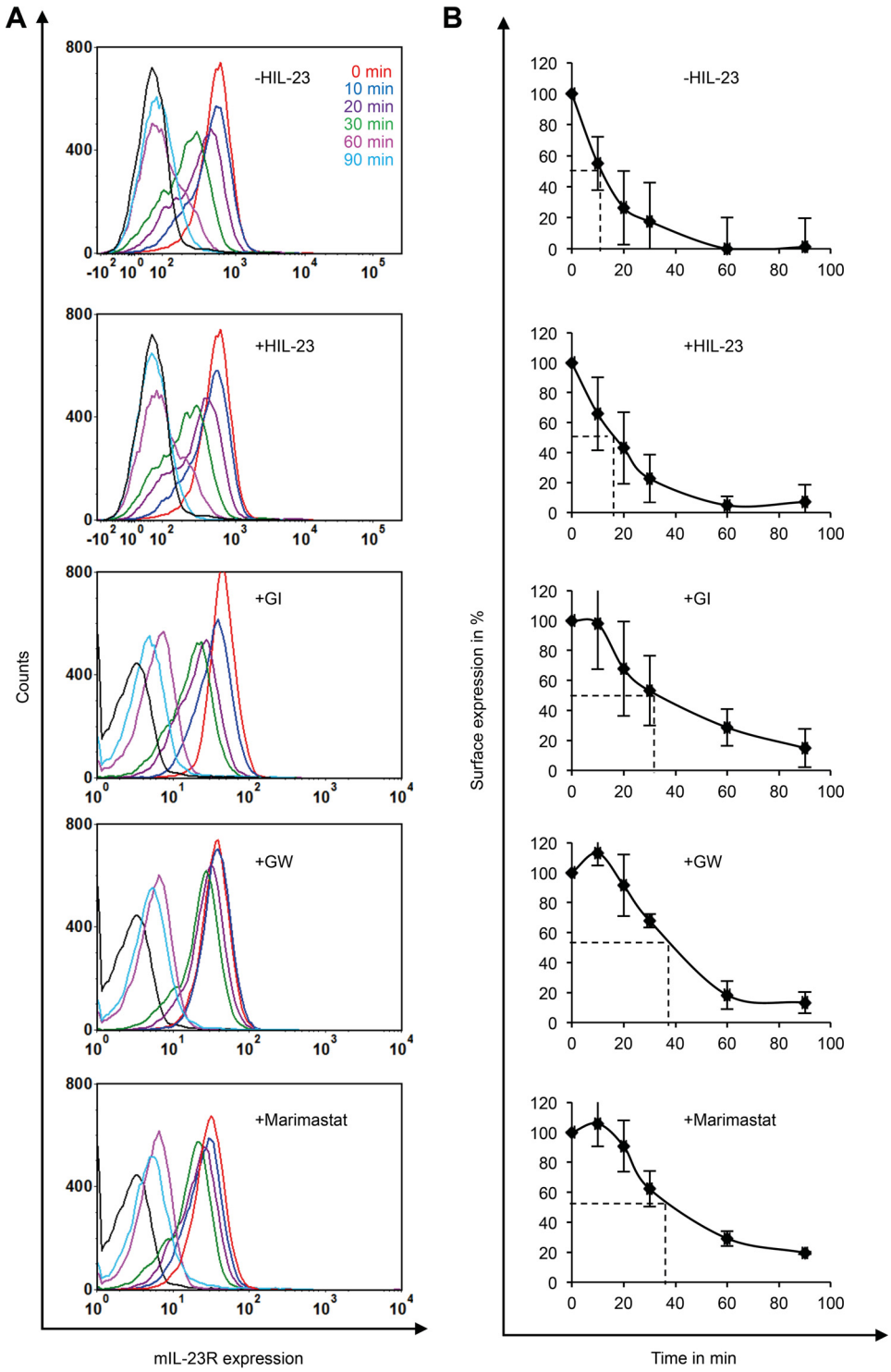

FIGURE 1. **Inhibition of ectodomain shedding prolonged the half-life of IL-23R on the cell surface.** *A*, murine IL-23R was antibody-labeled on Ba/F3-mIL-12Rβ1-mIL-23R cells that were preincubated by GI, GW, and Marimastat for 30 min at 37 °C. The cells were incubated with HIL-23 (0.2% conditioned supernatant) or Marimastat (10 μM), GI (3 μM), or GW (3 μM) at 37 °C for the indicated time points. Afterward the remaining receptor on the surface was stained by a fluorophore-coupled secondary antibody. Analysis of the remaining cell surface mIL-23R was made by flow cytometry. One representative example of three independent experiments is shown. *B*, the average of three independent experiments from *A* was calculated, and the cell surface mIL-23R expression was diagrammed after definition of time point 0 as 100%. The time point by which only 50% of the receptor was lost from the cell surface was calculated by mathematical calculation (best fit curve equation).

wild-type IL-23R situation (Fig. 3*C*), whereas shedding of mIL-23RΔ333–372 was almost completely abrogated (Fig. 3*C*), suggesting that the ADAM17 cleavage side was located in the area of the amino acid residues 333–342 of the murine IL-23R. Next, shedding of comparable deletion variants of the human IL-23R was analyzed. Therefore, we analyzed hIL-23R shedding in HEK293 cells. In detail, hIL-23RΔ344–353, hIL-23RΔ334–353, and hIL-23RΔ323–353 were generated (Fig. 3*D*), and

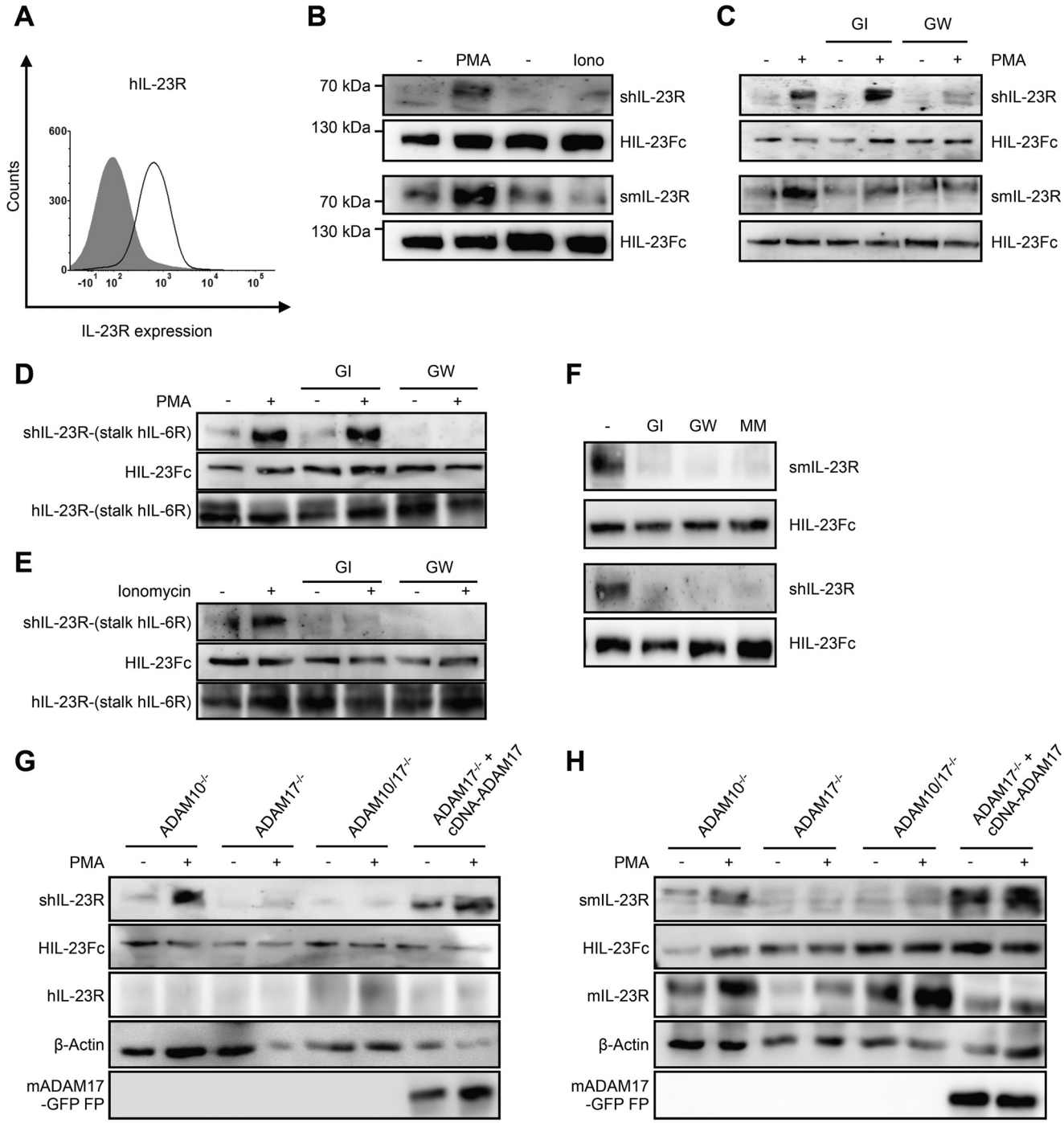

FIGURE 2. **Induced shedding of human and murine IL-23R is mediated by ADAM17.** *A*, cell surface expression analysis of human IL-23R on Ba/F3-gp130-hIL-12Rβ1-hIL-23R cells by flow cytometry. *B*, Ba/F3-hIL-12Rβ1-hIL-23R cells were incubated for 2 h with PMA (100 nM) or for 1 h with ionomycin (*Iono*, 1 μM). sIL-23R in the cellular supernatants was precipitated via HIL-23Fc/protein A-agarose and detected by Western blotting. Control cells were treated for 1 and 2 h with DMSO, which served as ionomycin/PMA solution reagent. *C*, a/F3-hIL-12Rβ1-hIL-23R and Ba/F3-mIL-12Rβ1-mIL-23R cells were treated with PMA, and sIL-23R was detected as in *B* in the presence and absence of GI (3 μM) or GW (3 μM). *D*, HEK293 cells were transiently transfected with a cDNA coding for hIL-23R-(stalk hIL-6R). The cells were treated with PMA, and sIL-23R-(stalk hIL-6R) was detected as in *B* in the presence and absence of GI (3 μM) or GW (3 μM). *E*, HEK293 cells were transiently transfected with a cDNA coding for hIL-23R-(stalk hIL-6R). The cells were treated with ionomycin, and sIL-23R-(stalk hIL-6R) was detected as in *B* in the presence and absence of GI (3 μM) or GW (3 μM). *F*, Ba/F3-gp130-hIL-12Rβ1-hIL-23R and Ba/F3-gp130-mIL-12Rβ1-mIL-23R cells were incubated for 24 h in the presence and absence of GI (3 μM), GW (3 μM), and Marimastat (*MM*, 10 μM). Human and murine sIL-23R were detected as in *B*. *G*, HEK293T cells deficient for ADAM10, ADAM17, or both and ADAM17-deficient HEK293 cells reconstituted with mADAM17 cDNA were transiently transfected with a cDNA coding for hIL-23R. The cells were treated with PMA and shIL-23R was detected as in *B*. Detection of cellular hIL-23R, β-actin, and mADAM17-GFP served as internal controls. *H*, HEK293T cells deficient for ADAM10, ADAM17, or both and ADAM17-deficient HEK293T cells reconstituted with mADAM17 were transiently transfected with a cDNA coding for mIL-23R. The cells were treated with PMA, and smIL-23R was detected as in *B*. Detection of cellular hIL-23R, β-actin, and mADAM17-GFP served as internal controls.

comparable expression of these variants in HEK293 cells was verified by Western blotting (Fig. 3*E*). Here, shedding of hIL-23RΔ344–353 and hIL-23RΔ334–353 after PMA stimulation was comparable with the wild-type IL-23R situation, whereas shedding of hIL-23RΔ323–353 was completely abrogated (Fig. 3*F*). These data suggest that the ADAM17 cleavage side was

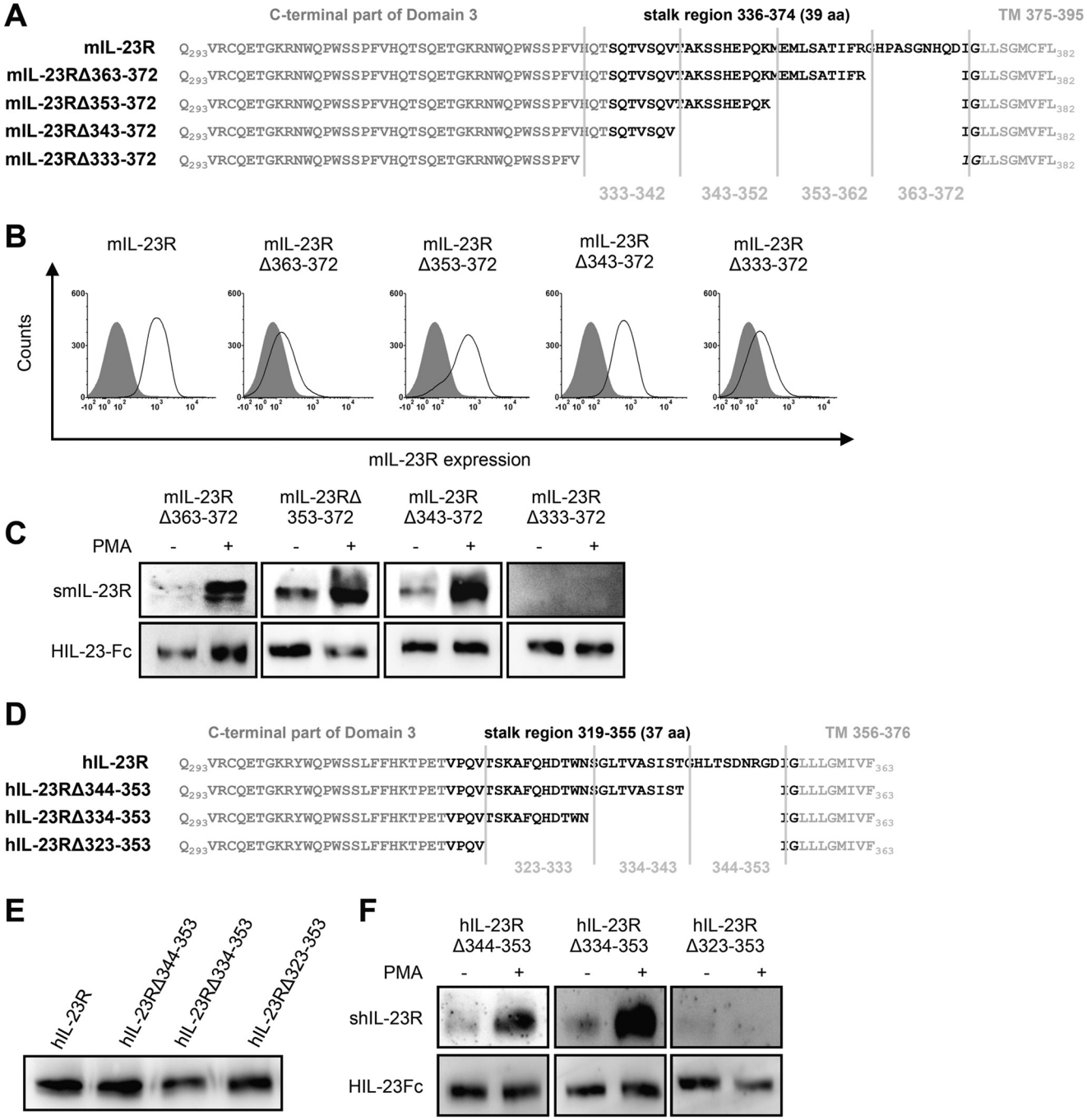

FIGURE 3. **Generation of noncleavable IL-23R variants by deletions within the stalk region of IL-23R.** *A*, amino acid sequence of the murine IL-23R and deletions thereof within the area of the stalk region, including the C-terminal end of domain 3 and the beginning of the transmembrane (*TM*) domain of the IL-23R. *B*, cell surface expression analysis of murine IL-23R and variants thereof in Ba/F3-gp130-mIL-12Rβ1-mIL-23R cells by flow cytometry. *C*, PMA-induced shedding of mIL-23RΔ363–372, mIL-23RΔ353–372, mIL-23RΔ343–372, and mIL-23RΔ333–372 in stably transduced Ba/F3-gp130-mIL-12Rβ1 cells. The cells were incubated for 2 h with PMA (100 nM). sIL-23R in the cellular supernatant was precipitated via HIL-23Fc and protein A-agarose and analyzed by Western blotting. Control cells were treated for 2 h with DMSO, which served as PMA solution reagent. *D*, amino acid sequence of the human IL-23R and deletions thereof within the area of the stalk region, including the C-terminal end of domain 3 and the beginning of the transmembrane domain of the IL-23R. *E*, expression analysis of hIL-23R and variants thereof in HEK293 cells was determined by Western blotting. *F*, PMA-induced shedding of mIL-23RΔ363–372, mIL-23RΔ353–372, mIL-23RΔ343–372, and mIL-23RΔ333–372 in transiently transfected HEK293 cells. The cells were incubated for 2 h with PMA (100 nM). sIL-23R in the cellular supernatant was precipitated via HIL-23Fc and protein A-agarose and analyzed by Western blotting. Control cells were treated for 2 h with DMSO, which served as PMA solution reagent.

located in the area of the amino acid residues 323–333 of the human IL-23R.

Homology alignment of predicted human and murine IL-23R stalk region revealed an overall low homology, except of the region 318–325 of the human IL-23R with 338–345 of the murine IL-23R (Fig. 4*A*, *boxed* amino acid residues). Although ADAM17 has no defined cleavage side, some prediction of preferred amino acids in the P1′ position can be made. ADAM17 prefers valine as amino acid in the P1′ position (24), and we identified two conserved valine residues at positions 339 and

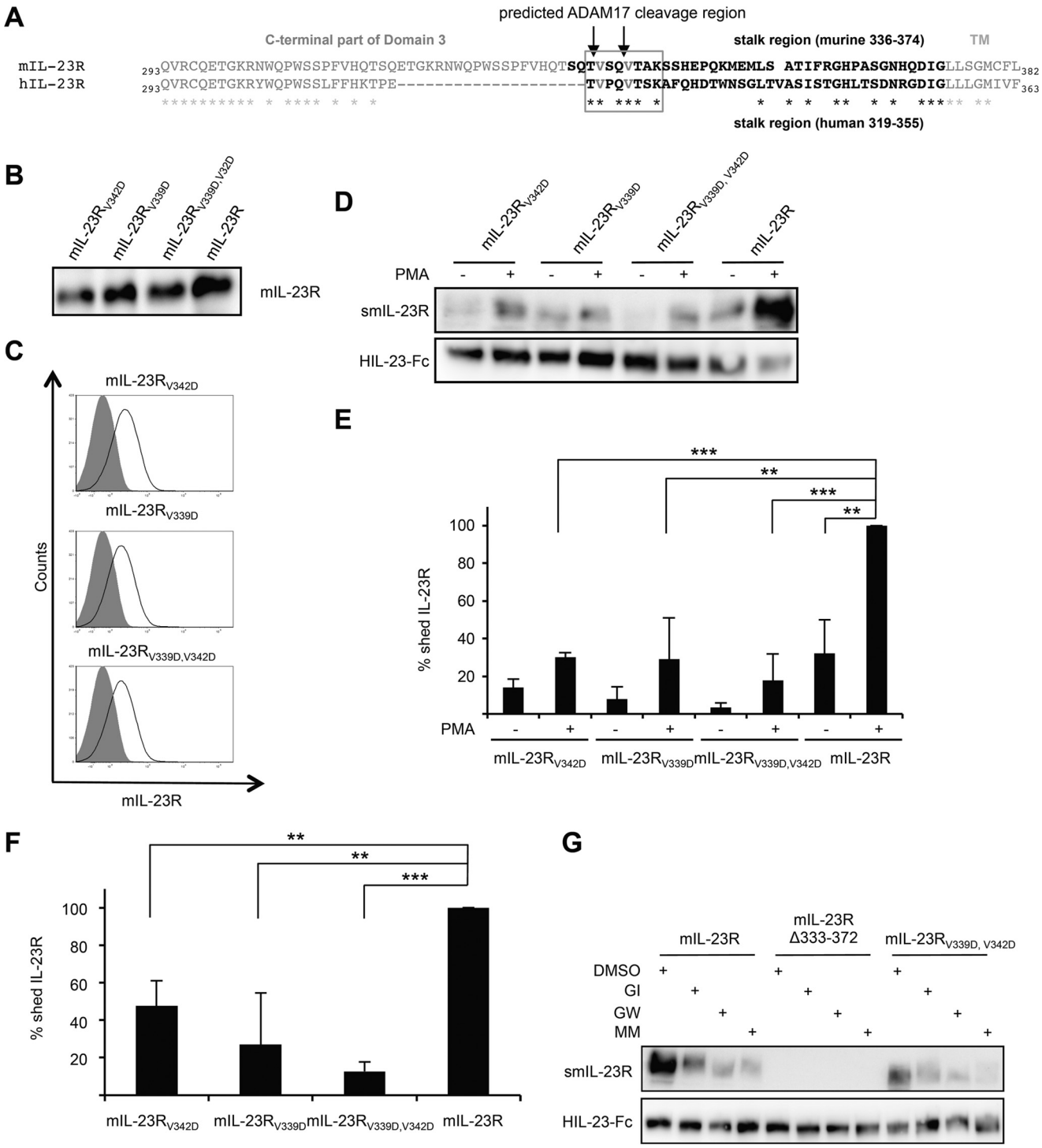

FIGURE 4. **Generation of noncleavable IL-23R variants by introduction of amino acid exchanges within the stalk region of IL-23R.** *A*, amino acid homology alignment of the human IL-23R within the area of the stalk region, including the C-terminal end of domain 3 and the beginning of the transmembrane (*TM*) domain of the IL-23R. *B* and *C*, expression analysis of mIL-23R, mIL-23R$_{V342D}$, mIL-23R$_{V339D}$, and mIL-23R$_{V339D/V342D}$ in stably transduced Ba/F3-gp130-mIL-12Rβ1 cells was determined by Western blotting (*B*) and flow cytometry (*C*). *D*, PMA-induced shedding of mIL-23R, mIL-23R$_{V342D}$, mIL-23R$_{V339D}$, and mIL-23R$_{V339D/V342D}$ in stably transduced Ba/F3-gp130-mIL-12Rβ1 cells was compared by Western blotting. *E*, the relative amount of PMA-induced shedding of sIL-23R as shown in *D* from three independent IL-23R shedding experiments as analyzed by Western blotting was quantified by ImageJ. *F*, the relative amount of constitutively shed sIL-23R as shown in *D* from three independent IL-23R shedding experiments as analyzed by Western blotting was quantified by ImageJ. *G*, constitutive shedding of mIL-23R, mIL-23RΔ333–372, and mIL-23R$_{V339D/V342D}$ in stably transduced Ba/F3-gp130-mIL-12Rβ1 cells was analyzed by Western blotting. Shedding was inhibited by GI (3 μM), GW (3 μM) and Marimastat (*MM*, 10 μM).

342 in the murine IL-23R and at positions 320 and 323 in the human IL-23R. Next, we introduced point mutations in the mIL-23R and replaced valine 339 and valine 342 to aspartic acid, which was the most unfavorable amino acid residue at P1′ for ADAM17. Cell surface expression of mIL-23R$_{V342D}$, mIL-23R$_{V339D}$, and the double mutant mIL-23R$_{V339D/V342D}$ was comparable in Ba/F3-gp130-mIL-12Rβ1 cells as verified by Western blotting and flow cytometry (Fig. 4, *B* and *C*).

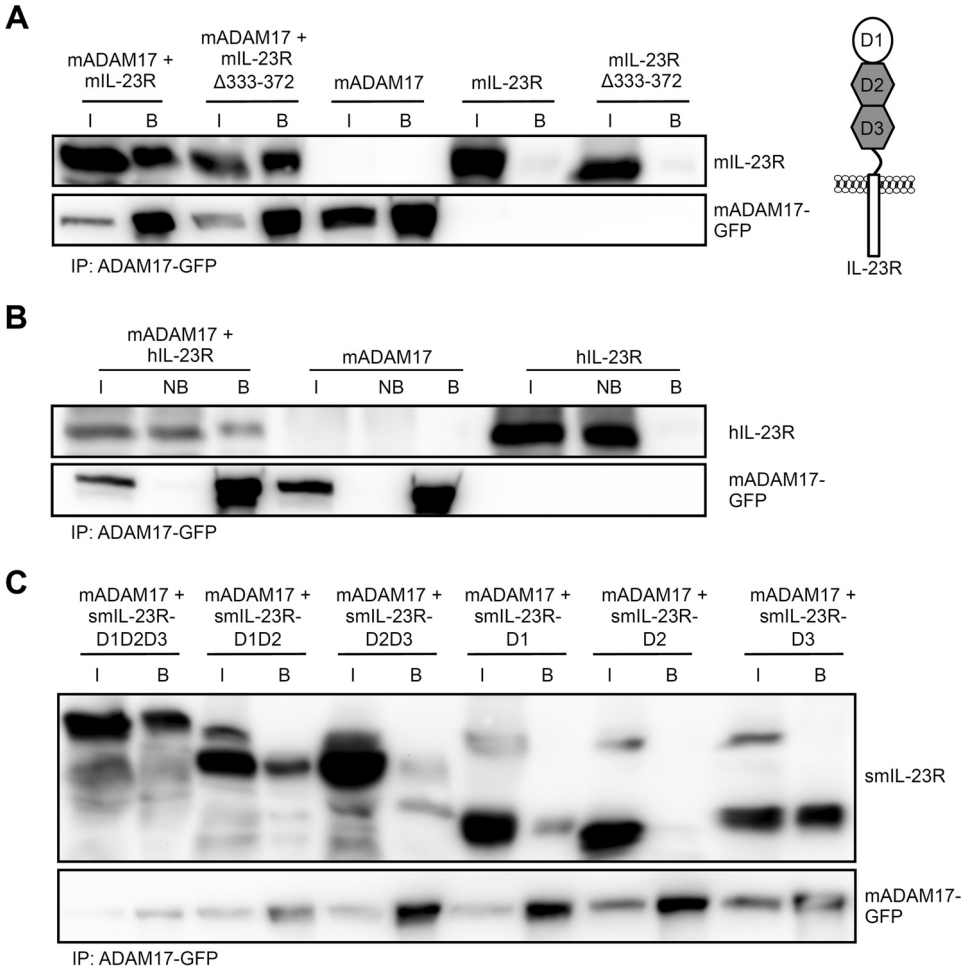

FIGURE 5. **Interaction of IL-23R with ADAM17 is mainly mediated by domain 1 and 3 of IL-23R.** *A*, *left panel*, cDNAs coding for mIL-23R and mADAM17-GFP were co-transfected in HEK293 cells. 48 h after transfection, the cells were lysed and precipitated by GFP nanobody Sepharose. mIL-23R and mADAM17-GFP were detected by Western blotting using mIL-23R and GFP antibodies. *Right panel*, schematic illustration of IL-23R domain structure. *B*, cDNAs coding for hIL-23R and mADAM17-GFP were co-transfected in HEK293 cells and interaction of IL-23R and mADAM17-GFP was analyzed as in *A*. *C*, cDNAs coding for smIL-23R and variants thereof with mADAM17-GFP were co-transfected in HEK293 cells, and interaction of smIL-23R and variants thereof with mADAM17-GFP was analyzed as in *A*. *I*, input; *NB*, nonbound after precipitation; *B*, bound after precipitation; *I*, immunoprecipitation.

Although some residual shedding of mIL-23R$_{V342D}$, mIL-23R$_{V339D}$, and the double mutant mIL-23R$_{V339D/V342D}$ was detected, it was greatly reduced as compared with wild-type murine IL-23R (Fig. 4*D*). Using ImageJ for quantification of Western blots from three independent experiments, our data indicate that shedding of all variants was significantly reduced by ~70–80% as compared with wild-type IL-23R (Fig. 4*E*). Interestingly, not only PMA-induced shedding but also constitutive shedding was significantly reduced (Fig. 4, *F* and *G*), suggesting that these amino acid residue exchanges also compromised constitutive shedding of the mIL-23R by ADAM10.

Interaction of IL-23R with ADAM17 Is Mainly Mediated by Domains 1 and 3 of IL-23R—Interaction of mADAM17 and mIL-23R was analyzed using a C-terminal fusion protein of mADAM17 with GFP and membrane-bound mIL-23R. GFP-tagged mADAM17 was precipitated with a GFP nanobody coupled to Sepharose (22). Transiently transfected HEK293 cells were co-transfected with cDNAs coding for mADAM17-GFP and mIL-23R. After lysis of the cells, mIL-23R and the non-cleavable mIL-23RΔ333–372 variant were co-precipitated with ADAM17-GFP (Fig. 5*A*), demonstrating that both proteins formed a complex, which was not depending on the cleaving capability of the substrate. As a control, IL-23R and the mIL-23RΔ333–372 variant were not precipitated by the GFP nanobody in the absence of ADAM17-GFP (Fig. 5*A*). Also human IL-23R was co-precipitated by mADAM17-GFP and GFP nanobody-Sepharose (Fig. 5*B*). Next, soluble variants of mIL-23R fused to an Fc domain from an IgG1 antibody were co-precipitated by mADAM17-GFP to identify the responsible domain within the mIL-23R for mADAM17 complex formation. Here, we generated soluble mIL-23R-Fc fusion proteins composed of all extracellular domains 1–3 (aa 24–315) lacking the stalk region of the IL-23R named smIL-23R-D1D2D3, of domains D1 and D2 (smIL-23R-D1D2, aa 24–217), of domains D2 and D3 (smIL-23R-D2D3, aa 122–315), and of only one of the domains (smIL-23R-D1, aa 24–123; smIL-23R-D2, aa 122–217; an smIL-23R-D3, aa 220–315). After co-transfection of cDNAs coding for sIL-23-Fc variants with mADAM17-GFP, cells were lysed and incubated with GFP nanobody Sepharose. Interestingly, smIL-23R-D1D2D3 was co-precipitated by mADAM17-GFP, demonstrating that the interaction of IL-23R and ADAM17 is mediated by the extracellular domains

of both proteins. Interestingly, binding was also shown for smIL-23R-D1D2 and, although to a lesser extent, by smIL-23R-D2D3. Confusingly, ADAM17 efficiently precipitated mIL-23R-D3, to a lesser extent mIL-23R-D1 but not IL-23R-D2 (Fig. 5*C*). Western blotting against the GFP tag of mADAM17 verified efficient precipitation of mADAM17-GFP. Our results demonstrate that the interaction of smIL-23R and mADAM17 is mainly mediated by domains 1 and 3 of the mIL-23R.

Discussion

Here, we describe that the murine and human IL-23R were substrates of the ADAM proteases ADAM10 and ADAM17. Initially, we found that the cell surface half-life of murine IL-23R was prolonged after broad spectrum inhibition of metalloproteases by Marimastat, suggesting ectodomain shedding of IL-23R. Because commercially available ELISAs were not sensitive enough to detect sIL-23R in cell culture supernatants, we made use of recombinant Fc-tagged Hyper-IL-23 to co-immunoprecipitate sIL-23R, followed by Western blotting of sIL-23R. Detailed analysis showed that ADAM17 cleaved IL-23R after stimulation with the phorbol ester PMA, whereas ADAM10 was responsible for constitutive shedding of the IL-23R but surprisingly not able to shed IL-23R after ionomycin treatment. To determine the responsible ADAM proteases, we made use of selective chemical inhibitors of ADAM10 und ADAM17 and HEK293 cells in which ADAM10/ADAM17 were genetically inactivated by CRISPR/Cas9. Exchange of the stalk region of the IL-23R by the IL-6R renders the synthetic IL-23R-(stalk-IL-6R) variant also sensitive for ionomycin-inducible ADAM10-mediated shedding. Co-immunoprecipitation of sIL-23R by IL-23 also showed that sIL-23R was biologically active in terms of IL-23 binding. We also tested whether the released sIL-23R was able to inhibit IL-23 signaling; however, the amount of sIL-23R in the cell culture supernatant was too low to inhibit IL-23 signaling (data not shown). Cleavage of ADAM proteases mostly occurs in the membrane-proximal region (11); stepwise deletion of the stalk region of the IL-23R, however, failed to determine a membrane-proximal target cleavage sequence within the IL-23R. Instead deletion of the complete stalk region suppressed constitutive and inducible shedding of IL-23R. Homology alignment of murine and human IL-23R revealed an overall low homology of the stalk region. Interestingly, a short amino acid stretch close to the domain 3 of IL-23R was highly conserved. Here, we identified two possible cleavage sites within the IL-23R. Mutation of two valines, which are preferred P1′ amino acids of ADAM17 cleavage (24), resulted in IL-23R variants, in which constitutive and induced shedding was dramatically reduced, suggesting that this was the cleavage site for ADAM10 and ADAM17 or that this region was critically involved in substrate recognition.

Human IL-23R is mainly expressed on activated memory T cells, natural killer cells, and innate lymphoid cells and at lower levels on monocytes, macrophages, and dendritic cells (25). Interestingly, no study directly approved cell surface expression of endogenous IL-23R by flow cytometry or Western blotting. We were, however, also not able to detect endogenous IL-23R on these cells, and therefore, our study lacks the direct proof that endogenous IL-23R is also a target of ADAM proteases.

Binding of ADAM proteases to substrates is considered to be mediated not via the cleavage site. First, we showed by co-immunoprecipitation that ADAM17 and murine and human IL-23R physically interact and that the putative cleavage site of the murine IL-23R was not needed for this interaction. Interestingly, smIL-23-D1D2D3 only consisting of the extracellular domains 1–3 was also efficiently co-immunoprecipitated by ADAM17, demonstrating also that the intracellular domain, the transmembrane domain, and the complete stalk region of IL-23R were not needed for substrate binding. Expression of single and combined extracellular domains of IL-23R showed, that ADAM17 interacts, although to a lesser extent with smIL-23-D1D2 and smIL-23-D2D3 and the single domains smIL-23R-D1 and smIL-23R-D3, but not with smIL-23-D2.

Alternative splicing of IL-23R result in a series of truncated soluble IL-23R proteins (12–14). Soluble variants of the IL-23R, lacking the transmembrane and intracellular region, represent potential therapeutic agents for the selective blockade of IL-23 signal transduction. Recombinant soluble IL-23R variants have been shown to block IL-23 and inhibit the generation of T_H17 cells (26, 27). Furthermore administration of a human soluble IL-23R protein protected mice against the development of EAE (26).

Here, we provide first evidence that IL-23R is a substrate of ectodomain shedding. Shedding of IL-23R might contribute to negative regulation of IL-23 signaling with two major steps. First, ectodomain shedding of IL-23R result in down-regulation of cell surface expressed IL-23R molecules and thereby might reduce the cellular responsiveness toward IL-23. Second, sIL-23R is able to bind to IL-23 and thereby might act as competitive antagonist of IL-23 signaling.

Author Contributions—M. F., D. M. F., and J. S. designed the study. M. F., J. S., N. M., T. A., and T. M. H. performed experiments. B. R., C. G., and C. B.-P. provided materials and discussed the data. M. F., D. M. F., and J. S. contributed to drafting the manuscript.

Acknowledgment—We thank Esther van de Vosse (Leiden University Medical Center, Leiden, The Netherlands) for cDNAs for IL-23R and IL-12Rβ1.

References

1. Floss, D. M., Schröder, J., Franke, M., and Scheller, J. (2015) Insights into IL-23 biology: from structure to function. *Cytokine Growth Factor Rev.* **26,** 569–578
2. Ouyang, W., Kolls, J. K., and Zheng, Y. (2008) The biological functions of T helper 17 cell effector cytokines in inflammation. *Immunity* **28,** 454–467
3. Cosmi, L., Maggi, L., Santarlasci, V., Liotta, F., and Annunziato, F. (2014) T helper cells plasticity in inflammation. *Cytometry A* **85,** 36–42
4. Presky, D. H., Yang, H., Minetti, L. J., Chua, A. O., Nabavi, N., Wu, C. Y., Gately, M. K., and Gubler, U. (1996) A functional interleukin 12 receptor complex is composed of two β-type cytokine receptor subunits. *Proc. Natl. Acad. Sci. U.S.A.* **93,** 14002–14007
5. Parham, C., Chirica, M., Timans, J., Vaisberg, E., Travis, M., Cheung, J., Pflanz, S., Zhang, R., Singh, K. P., Vega, F., To, W., Wagner, J., O'Farrell, A. M., McClanahan, T., Zurawski, S., *et al.* (2002) A receptor for the heterodimeric cytokine IL-23 is composed of IL-12Rβ1 and a novel cytokine receptor subunit, IL-23R. *J. Immunol.* **168,** 5699–5708
6. Schröder, J., Moll, J. M., Baran, P., Grötzinger, J., Scheller, J., and Floss,

D. M. (2015) Non-canonical interleukin 23 receptor complex assembly: p40 protein recruits interleukin 12 receptor β1 via site II and induces p19/interleukin 23 receptor interaction via site III. *J. Biol. Chem.* **290,** 359–370
7. Floss, D. M., Mrotzek, S., Klöcker, T., Schröder, J., Grötzinger, J., Rose-John, S., and Scheller, J. (2013) Identification of canonical tyrosine-dependent and non-canonical tyrosine-independent STAT3 activation sites in the intracellular domain of the interleukin 23 receptor. *J. Biol. Chem.* **288,** 19386–19400
8. Edwards, D. R., Handsley, M. M., and Pennington, C. J. (2008) The ADAM metalloproteinases. *Mol. Aspects Med.* **29,** 258–289
9. Garbers, C., Jänner, N., Chalaris, A., Moss, M. L., Floss, D. M., Meyer, D., Koch-Nolte, F., Rose-John, S., and Scheller, J. (2011) Species specificity of ADAM10 and ADAM7 in IL-6 transsignaling and novel role of ADAM10 in inducible IL-6R shedding. *J. Biol. Chem.* **286,** 14804–14811
10. Le Gall, S. M., Bobé, P., Reiss, K., Horiuchi, K., Niu, X. D., Lundell, D., Gibb, D. R., Conrad, D., Saftig, P., and Blobel, C. P. (2009) ADAMs 10 and 17 represent differentially regulated components of a general shedding machinery for membrane proteins such as transforming growth factor α, L-selectin, and tumor necrosis factor α. *Mol. Biol. Cell* **20,** 1785–1794
11. Scheller, J., Chalaris, A., Garbers, C., and Rose-John, S. (2011) ADAM17: a molecular switch controlling inflammatory and regenerative responses. *Trends Immunol* **32,** 380–387
12. Kan, S. H., Mancini, G., and Gallagher, G. (2008) Identification and characterization of multiple splice forms of the human interleukin-23 receptor α chain in mitogen-activated leukocytes. *Genes Immun* **9,** 631–639
13. Mancini, G., Kan, S. H., and Gallagher, G. (2008) A novel insertion variant of the human IL-23 receptor-α chain transcript. *Genes Immun* **9,** 566–569
14. Zhang, X. Y., Zhang, H. J., Zhang, Y., Fu, Y. J., He, J., Zhu, L. P., Wang, S. H., and Liu, L. (2006) Identification and expression analysis of alternatively spliced isoforms of human interleukin-23 receptor gene in normal lymphoid cells and selected tumor cells. *Immunogenetics* **57,** 934–943
15. Fischer, M., Goldschmitt, J., Peschel, C., Brakenhoff, J. P., Kallen, K. J., Wollmer, A., Grötzinger, J., and Rose-John, S., (1997) A bioactive designer cytokine for human hematopoietic progenitor cell expansion. *Nat. Biotechnol.* **15,** 142–145
16. Hundhausen, C., Misztela, D., Berkhout, T. A., Broadway, N., Saftig, P., Reiss, K., Hartmann, D., Fahrenholz, F., Postina, R., Matthews, V., Kallen, K. J., Rose-John, S., and Ludwig, A. (2003) The disintegrin-like metalloproteinase ADAM10 is involved in constitutive cleavage of CX3CL1 (fractalkine) and regulates CX3CL1-mediated cell-cell adhesion. *Blood* **102,** 1186–1195
17. de Paus, R. A., van de Wetering, D., van Dissel, J. T., and van de Vosse, E. (2008) IL-23 and IL-12 responses in activated human T cells retrovirally transduced with IL-23 receptor variants. *Mol. Immunol.* **45,** 3889–3895
18. van de Vosse, E., de Paus, R. A., van Dissel, J. T., and Ottenhoff, T. H. (2005) Molecular complementation of IL-12Rβ1 deficiency reveals functional differences between IL-12Rβ1 alleles including partial IL-12Rβ1 deficiency. *Hum. Mol. Genet.* **14,** 3847–3855
19. Althoff, K., Reddy, P., Voltz, N., Rose-John, S., and Müllberg, J. (2000) Contribution of the amino acid sequence at the cleavage site to the cleavage pattern of transmembrane proteins. *Eur. J. Biochem.* **267,** 2624–2631
20. Suthaus, J., Tillmann, A., Lorenzen, I., Bulanova, E., Rose-John, S., and Scheller, J. (2010) Forced homo- and heterodimerization of all gp130-type receptor complexes leads to constitutive ligand-independent signaling and cytokine-independent growth. *Mol. Biol. Cell* **21,** 2797–2807
21. Oppmann, B., Lesley, R., Blom, B., Timans, J. C., Xu, Y., Hunte, B., Vega, F., Yu, N., Wang, J., Singh, K., Zonin, F., Vaisberg, E., Churakova, T., Liu, M., Gorman, D., *et al.* (2000) Novel p19 protein engages IL-12p40 to form a cytokine, IL-23, with biological activities similar as well as distinct from IL-12. *Immunity* **13,** 715–725
22. Rothbauer, U., Zolghadr, K., Muyldermans, S., Schepers, A., Cardoso, M. C., and Leonhardt, H. (2008) A versatile nanotrap for biochemical and functional studies with fluorescent fusion proteins. *Mol. Cell. Proteomics* **7,** 282–289
23. Garbers, C., Monhasery, N., Aparicio-Siegmund, S., Lokau, J., Baran, P., Nowell, M. A., Jones, S. A., Rose-John, S., and Scheller, J. (2014) The interleukin-6 receptor Asp358Ala single nucleotide polymorphism rs2228145 confers increased proteolytic conversion rates by ADAM proteases. *Biochim. Biophys. Acta* **1842,** 1485–1494
24. Tucher, J., Linke, D., Koudelka, T., Cassidy, L., Tredup, C., Wichert, R., Pietrzik, C., Becker-Pauly, C., and Tholey, A. (2014) LC-MS based cleavage site profiling of the proteases ADAM10 and ADAM17 using proteome-derived peptide libraries. *J. Proteome Res.* **13,** 2205–2214
25. Ngiow, S. F., Teng, M. W., and Smyth, M. J. (2013) A balance of interleukin-12 and -23 in cancer. *Trends Immunol* **34,** 548–555
26. Guo, W., Luo, C., Wang, C., Zhu, Y., Wang, X., Gao, X., and Yao, W. (2012) Protection against Th17 cells differentiation by an interleukin-23 receptor cytokine-binding homology region. *PLoS One* **7,** e45625
27. Yu, R. Y., and Gallagher, G. (2010) A naturally occurring, soluble antagonist of human IL-23 inhibits the development and *in vitro* function of human Th17 cells. *J. Immunol.* **185,** 7302–7308
28. Cho, M. L., Kang, J. W., Moon, Y. M., Nam, H. J., Jhun, J. Y., Heo, S. B., Jin, H. T., Min, S. Y., Ju, J. H., Park, K. S., Cho, Y. G., Yoon, C. H., Park, S. H., Sung, Y. C., and Kim, H. Y. (2006) STAT3 and NF-κB signal pathway is required for IL-23-mediated IL-17 production in spontaneous arthritis animal model IL-1 receptor antagonist-deficient mice. *J. Immunol.* **176,** 5652–5661